Published in final edited form as:
Biomaterials. 2015 January ; 37: 156–163. doi:10.1016/j.biomaterials.2014.10.022.

Spatiotemporal dynamics of microRNA during epithelial collective cell migration

Zachary S. Dean[a], **Reza Riahi**[b,1], and **Pak Kin Wong**[a,b,c,*]

[a]Biomedical Engineering Interdisciplinary Program, The University of Arizona, Tucson, AZ 85721-0119, USA

[b]Department of Aerospace and Mechanical Engineering, The University of Arizona, Tucson, AZ 85721-0119, USA

[c]BIO5 Institute, The University of Arizona, Tucson, AZ 85721-0119, USA

Abstract

MicroRNAs (miRNAs) are small, noncoding RNAs variably involved in a wide variety of developmental and regenerative programs. Techniques for monitoring the spatiotemporal expression of miRNA in living cells are essential to elucidate the roles of miRNA during these complex regulatory processes. The small size, low abundance, sequence similarity, and degradation susceptibility of miRNAs, however, make their detection challenging. In this study, we detail a double-stranded locked nucleic acid (dsLNA) probe for detecting intracellular miRNAs during epithelial collective migration. The dsLNA probe is capable of detecting the dynamic regulation and dose-dependent modulation of miRNAs. The probe is applied to monitor the spatial distribution of miRNA expression of a migrating epithelium. Our results reveal a gradient of miRNA over the first one hundred microns from the leading edge and show the involvement of miR-21 in the complex regulation of transforming growth factor beta modulated epithelial migration. With its ease of use and capacity for real-time monitoring of miRNAs in living cells, the dsLNA probe carries the potential for studying the function and regulation of miRNA in a wide spectrum of complex biological processes.

Keywords

microRNA; single cell; collective migration; TGF-β; intracellular detection

*Corresponding author. Tel: +1-520-626-2215; Fax: 1-520-621-8191; pak@email.arizona.edu.
[1]Current address: Harvard-MIT Health Sciences and Technology, Massachusetts Institute of Technology and Harvard Medical School, Cambridge, MA 02139, USA

1. Introduction

MicroRNAs (miRNAs) are a ubiquitous class of small (19–25 nucleotides), endogenous, non-coding RNAs that coordinate post-transcriptional regulation of gene expression. Mature miRNAs, in concert with the RNA-induced silencing complex (RISC), combine with the 3′ untranslated region of target mRNAs, triggering either the degradation or translational inhibition of the target mRNA. Over 17,000 miRNAs throughout more than 140 species have been documented and dynamic miRNA expression profiles have been recognized for varying physiological and pathological conditions [1]. In particular, miRNAs are implicated in a variety of cellular processes, such as tissue development, wound healing, and cancer metastasis [2, 3]. miR-21 and -23b, for instance, were shown to regulate collective migration and invasion of epithelial cells with opposing effects; miR-21 is implicated in increased migration, while miR-23b is involved in migration suppression [3–5]. miRNA levels during these operations have been known to be modulated by different cytokines, such as transforming growth factor β (TGF-β) [6, 7].

The nature of miRNAs makes their detection difficult: short length, low quantity, sequence similarity, and susceptibility to degradation [8]. While a wide variety of miRNA detection methods exist, many of the current techniques are not suitable for detecting the diverse distribution of miRNA levels in complex biological experiments, such as collective cell migration and epithelial-mesenchymal transition. Northern blot RNA analysis, for instance, is not only tedious and time-consuming, but also requires a larger quantity of miRNA. Quantitative RT-PCR has better sensitivity; however, specific probe design for miRNA is difficult due to the small length and similar sequences between related miRNAs. *In situ* hybridization can determine spatial miRNA distribution, but it is technically challenging. More importantly, monitoring miRNA expression over time with conventional RNA measurement techniques is demanding due to the requirement of cell fixation or lysis [9].

We have previously demonstrated a double-stranded locked nucleic acid (dsLNA) probe for detecting spatiotemporal changes of mRNA in living cells [10–13]. The dsLNA probe incorporates a donor fluorophore on the 5′ end of one strand with an adjacent quencher molecule on the 3′ end of the complementary strand. Functionally, the dsLNA probe exists in two states. In the absence of target RNA, the donor and quencher strands remain in close proximity, and the probe's fluorescence signal is suppressed. In the presence of RNA target, however, the donor strand preferably binds to the target as opposed to the quencher due to a thermodynamic binding event, and the probe's signal can be measured via fluorescence measurement (Fig. 1a). To enable real-time monitoring of RNA expression in living cells, the probe should produce fluorescence only in the presence of a specific target sequence (Fig. 1b) [14–16]. The standard oligonucleotide probe phosphate deoxyribose backbone composition, however, is largely susceptible to single-strand binding proteins and nuclease degradation, requiring modification to prevent false-positive signals. Of these modifications, 2′-sugar modifications, such as locked nucleic acids (LNA), are some of the most effective RNA-binding oligonucleotides due to their increased binding affinity and resistance to degradation [17–19]. In particular, alternating DNA/LNA bases has been shown to not only optimize the balance between specificity and stability for intracellular detection, but it has

also proven accurate enough to distinguish gene expression in a population of cells down to the single-cell level [10, 20].

In the present study, we investigate the applicability of dsLNA probes for detecting spatiotemporal changes of miRNA during epithelial collective migration. Probes targeting β-actin mRNA, miR-21, miR-23b, and a random negative control probe are designed and optimized for maximal target binding affinity. The ability of the dsLNA probe to detect miR-21 and miR-23b levels is examined in MCF-7 epithelial cancer cells by measuring the probe's response to TGF-β, an anti-proliferative cytokine that plays important roles in collective cell migration and epithelial-mesenchymal transition [21, 22]. TGF-β increases mature miR-21 through Dicer splicing of pri-miR-21 to pre-miR-21, as well as inhibits miR-23b expression at the transcriptional level [23, 24]. The induction of miRNA by TGF-β in MCF-7 cells is monitored dynamically to study the dynamics of miRNA levels. To investigate the roles of miRNA in the regulation of epithelial collective migration, the distributions of miRNA are monitored in model wounds of MCF-7 cells with and without the addition of TGF-β.

2. Materials and methods

2.1 Probe design and preparation

The dsLNA probe is composed of two oligonucleotide strands with alternating DNA and LNA monomers. The donor strand is twenty nucleotides long and designed complementary to either the target mRNA or miRNA of interest. The fluorophore used for fluorescence detection, 6-FAM, is located at the 5′ end of the donor strand. The second strand of the dsLNA probe, the quencher strand, is ten nucleotides in length. A dark quencher, Iowa Black FQ, is located at the 3′ end of the quenching strand immediately adjacent to the donor fluorophore on the donor strand.

Four dsLNA probes were developed for spatiotemporal gene expression analysis in this study (Table 1). A probe targeting β-actin mRNA was designed, and the sequence was verified using the NCBI GenBank database. A random, scrambled probe was developed with no known intracellular targets as a negative control. The sequences of both the β-actin and random probe sequences were also additionally verified through NCBI Basic Local Alignment Search Tool for nucleotide sequences (BLASTn). The miR-21 and miR-23b probes were similarly designed, but the sequences were verified using miRBase's sequence database [1]. The probes were prepared for transfection by dissolving the donor and quencher strands in 10 mM Tris-EDTA buffer and 0.2 M NaCl before mixing them at a 1:2 molar ratio, respectively. The probes were then heated at 95°C for five minutes in a dry bath incubator before cooling to room temperature gradually over the course of two and a half hours.

2.2 Cell culture and transfection

MCF-7 human mammary gland adenocarcinoma was obtained from American Type Culture Collection (Manassas, VA). The cells were grown in Dulbecco's Modified Eagle Medium (Corning, Manassas, VA) supplemented with 10% fetal bovine serum (Corning, Manassas, VA), 1% L-glutamine (Sigma-Aldrich, St. Louis, MO), and 0.1% gentamycin (Sigma-

Aldrich, St. Louis, MO). Cells were incubated at 37°C and 5% CO_2 in a tissue culture incubator. Cells were grown to 90–95% confluence in a 24-well plate before transfection in order to study the dose-dependent expression of miR-21 and miR-23b with TGF-β addition. The probe and Lipofectamine 2000 transfection reagent (Invitrogen, Carlsbad, CA) were combined according to the manufacturer's protocol prior to transfection. 0.8 μg probe was transfected per well, with 2.4 μL Lipofectamine 2000 transfection reagent used per well.

2.3 Inducible miRNA expression

Experiments were performed to study the dsLNA probe's ability to detect inducible miRNA expression changes via TGF-β1 (R & D Systems, Minneapolis, MN). The MCF-7 cell medium was changed to serum-free medium six hours after seeding. Twenty-four hours later the medium was replaced with new serum-free medium, and the cells were transfected with either the miR-21 probe, the miR-23b probe, or the random scrambled probe, which served as a negative control. Twenty-four hours after adding the transfection reagents, the serum-free medium was again replaced and TGF-β was added at 1 ng/mL, 2 ng/mL, 5 ng/mL, or 10 ng/mL. To measure miR-21 over time, images were taken at 0, 1, 2, 4, and 24 hours after adding TGF-β. To measure the dose-dependent changes in miR-21 and miR-23b via TGF-β, the cells were incubated with TGF-β for twenty-four hours before images were taken. Cells were washed twice with PBS prior to acquiring images.

2.4 Wound healing assay for inducing epithelial migration

MCF-7 cells were seeded and grown to confluence before they were scratched with a 1000 μL Neptune Biotix traditional-shaped pipette tip [25]. The cells were immediately washed twice with serum-free media to remove dead cells then transfected as described above. Twenty-four hours after transfection, cells were either incubated for twenty-four hours with TGF-β (5ng/mL) or in the absence of TGF-β before measuring the spatial distribution of genes from the wound edge. Fluorescence images were taken twenty-four hours after TGF-β addition. Cells were allowed to migrate for 24 hours before wound closure rate was measured. A mark on the underside of the plates ensured that the same wound areas were measured. Six wells of a 24-well plate were measured for each condition, and at least two sections of each well were evaluated. For the proliferation experiments, Click-iT EdU (Invitrogen, Carlsbad, CA) was used according to manufacturer's protocol. As a control, 4 mM HCl with 1 mg/mL bovine serum albumin was utilized for the 0 ng/mL TGF-β scenarios (the TGF-β buffer). Migration rate was determined by measuring the area covered by the cells over 24 hours and dividing by the width of the monolayer.

2.5 Imaging and data analysis

Images were taken with an inverted fluorescence microscope (TE2000-U, Nikon) and acquired with a CCD camera (SensiCamQE, Cook Corp.). All fluorescence images were taken with the same exposure time for comparison purposes. Data analysis was performed using NIH ImageJ software [26], and approximately 200 cells were measured per well for each experiment except the wound healing experiments, where approximately 800 cells were measured per well. At least 3 samples were used per experiment. Experimental data were evaluated as mean ± SEM. The student's t-test was used in comparing two independent groups. For the comparison of multiple groups, a one-way ANOVA analysis was used with

the post hoc Tukey's multiple comparison test. $P < 0.05$ was accepted as statistically significant.

3. Results

3.1 Dose-dependent miRNA modulation by TGF-β

The probe transfection protocol was first optimized to maximize the transfection efficiency and the signal-to-noise ratio for intracellular miRNA detection. Transfection optimization is particularly important for miRNA detection due to the inherently low miRNA abundance in cells. In the experiment, the optimal donor-to-quencher ratio was 1-to-2, which resulted in a high signal-to-noise ratio (data not shown). The Lipofectamine 2000-to-probe ratio was adjusted by maintaining the probe transfection weight at 0.8 μg per well while varying the Lipofectamine 2000 volume. In a 24-well plate, the optimal transfection efficiency, as well as the most favorable signal-to-noise ratio, was achieved was 3.0 μL Lipofectamine 2000 per 500 μL culture media. Fig. S1 and S2 show the average fluorescence signal and transfection efficiency results. The transfection efficiency was defined as the percentage of cells with detectable cytoplasm fluorescence using the β-actin probes. Fig. 1c shows a representative image of cells transfected with the β-actin probes. To determine the transfection efficiency in cell populations, the distributions of miR-21 and random probes in MCF-7 monolayers were analyzed using GraphPad Prism 5 (Fig. S3). The variance of miR-21 was large compared to the variance of the random probe, suggesting the miR-21 expression is heterogeneous.

Following transfection optimization, the dsLNA probe's ability to distinguish the concentration of miRNA in live cells was tested. TGF-β, a cytokine which increases mature miR-21 and decreases miR-23b [23, 24], was added to MCF-7 cells in doses ranging from 0 ng/mL to 10 ng/mL. The miR-21 probe's signal with TGF-β addition can be visualized through the corresponding images in Fig. 2a. The miR-21 dsLNA probe's signal gradually increased as TGF-β concentrations escalated from 0 ng/mL to 10 ng/mL (Fig. 2b). Statistical analysis confirmed that the expression of miR-21 changed as TGF-β doses increased, with 2, 5, and 10 ng/mL TGF-β presenting significant increases ($P<0.001$) in miR-21 compared to the control. In contrast, the intensity of miR-23b probe decreased by roughly 30% compared to the basal intensity at 1 ng/mL TGF-β, and farther decreased to half of the basal intensity at all tested levels of TGF-β above 1 ng/mL (Fig. 2c). In contrast, the random probe showed no statistical difference ($P<0.05$) at all doses of TGF-β, whether compared with control (0 ng/mL TGF-β), or between groups (Fig. 2d). These results are in good agreement with previous miRNA studies in various cells types and conditions, supporting the applicability of the dsLNA probes for intracellular miRNA detection [24, 27].

3.2 Dynamic measurement of miR-21 after TGF-β addition

The dsLNA probe enables living cell gene expression dynamic monitoring. To study the probe's ability to measure fluctuations in miRNA levels over time, 10 ng/mL TGF-β was added to MCF-7 cells. Dynamic miR-21 shifts over time were compared to the random probe, which served as a control. Fig. 3a shows the bright-field and fluorescence images of the cells at different time points. The miR-21 level increased rapidly during the first 2 hours

of TGF-β incubation. At two hours, a 2.5-fold increase of the intensity was observed. At 24 hours after TGF-β addition, the intensity decreased slightly to a ratio of approximately 2. The measured dynamics and induction levels resembled reported values from previous TGF-β studies [28, 29]. To further verify that the observed dynamic miR-21 expression is induced by TGF-β, the experiment was repeated without TGF-β addition or with random probe (Fig. 3c and Fig. S4). Without TGF-β, miR-21 level did not change significantly over time, and regardless of TGF-β status the random probe signal also remained unchanged. An unpaired student's t-test showed that the difference between miR-21 and random probe signals remained statistically significant with and without TGF-β for all time points. Without TGF-β addition, no significant change in miR-21 was detected. In addition, the miR-21 expression increase over time was significant between the point of TGF-β addition to 1 hour after TGF-β addition (*, $P<0.05$), as well as between 1 to 2 hours after TGF-β addition (**, $P<0.01$). Importantly, the miR-21 signal remained statistically significant when compared to the random probe signal, regardless of time and regardless of TGF-β application (***, $P<0.001$). Taken together, the experiments demonstrate the dsLNA probe's ability to measure TGF-β modulation of miRNA in live cells and to perform dynamic miRNA measurements for twenty-four hours.

3.3 Spatial measurement of miRNA during epithelial collective migration

The dsLNA probe's single cell detection capability potentializes spatial RNA expression monitoring during epithelial collective cell migration. To study the dsLNA probe's ability to measure the spatial distribution of miRNA, MCF-7 epithelial cells were seeded in a 24-well plate and grown to confluence before a model wound was created in the monolayer with a pipette tip. β-actin mRNA has been previously shown to increase at the wound edge as the cells manage cell growth and migration [20]. The random control probe again signified the background level inherent in the experiment. Fig. 4a illustrates the leading edge of the monolayer for β–actin, miR-21 and random probes. The corresponding bright-field image for each fluorescence image was also included. Fig. 4b quantified the fluorescence intensity distribution from the leading edge of the wound back toward the monolayer. The β-actin mRNA signal was upregulated as much as 3-fold near the wound edge. A gradient of β-actin mRNA spanned approximately 100 μm from the wound edge before reaching basal level. The random probe, in contrast, did not increase at the wound edge or farther into the monolayer. The miR-21 probe, interestingly, also showed an increase in miR-21 at the wound edge for ~ 2-fold. Much like the β-actin probe, the increase occurred for roughly the first 100 μm from the wound edge before leveling off. To study the effects of TGF-β on the spatial distribution of miR-21 in the wound healing experiment, 5 ng/mL TGF-β was also added to the cells (Fig. 4b). Neither the random probe nor the β-actin probe experienced a significant increase in signal at any location from the wound edge, while the miR-21 probe was increased at all locations in the monolayer (Fig. S5). The miR-21 signal was particularly increased at the wound edge, where it was statistically increased over the first 40 μm (***, $P<0.001$). These results reveal miR-21 is spatially coordinated near the leading edge of a migrating epithelium and the spatial distribution of miR-21 correlates with the β-actin mRNA.

3.4 MCF-7 collective migration and spatial proliferation with TGF-β addition

The dsLNA probe exposed increased β-actin and miR-21 expression near the wound edge. Questions remained, however, regarding the effects of TGF-β and miR-21 on the migrating epithelium. To further investigate these questions, the migration and proliferation rates of MCF-7 cells near a model wound edge were measured (Fig. 5). For assessing migration, cells were allowed to travel into the cell-free region of the wound for twenty-four hours before their migration rate was estimated. To measure the spatial proliferation rate distribution of MCF-7 cells with and without TGF-β addition, the Click-iT EdU Imaging Kit was utilized according to manufacturer's protocol. The cells were allowed to proliferate in the presence or absence of TGF-β for twenty-four hours before fixation. Hoechst 33342 dye was used to determine the total cell count either at the wound edge or in 100 μm increments away from the monolayer. Proliferation was measured by comparing the fraction of cells expressing Alexa Fluor 488 azide (Fig. 5a).

Fig. 5b shows the proliferation rate at different locations with and without TGF-β. Cell proliferation was significantly decreased in the first 100 μm from the wound edge when compared to the cell proliferation further back in the monolayer in both the TGF-β and control conditions. The region with decreased proliferation correlated spatially with the areas of increased miRNA and β-actin expression. Furthermore, cell proliferation in response to TGF-β was consistently decreased, from four to nine percent, regardless of the cell's location in relation to the wound edge. The migration rates with and without TGF-β are shown in Fig. 5c. Cells treated with TGF-β were observed to migrate significantly slower than control cells.

4. Discussion

In this study, a dsLNA probe capable of measuring spatiotemporal dynamics of miRNA was presented. Alternating LNA-DNA nucleotides were incorporated into the probes, allowing for stable miRNA detection in living cells for over twenty-four hours, qualitative analysis of low copy-number RNAs, and dynamic miRNA expression monitoring after the chemical or physical stimulation of cells. TGF-β, which upregulates miR-21 expression as well as downregulates miR-23b expression [23, 24], was added to MCF-7 epithelial breast cancer cells. The results demonstrated that the dsLNA probes could measure the dose-dependent induction in miR-21 by TGF-β. An increase in miR-21 expression occurred up to a dose of 10 ng/mL TGF-β, where the miR-21 level was 2.5-fold greater than the basal level. These results are in good agreement in previous studies of miR-21 [27]. To further verify the dsLNA probe's ability to detect inducible changes in miRNA levels, a second miRNA, miR-23b, was observed to decrease in a dose-dependent fashion via TGF-β addition. The signal intensity of the dsLNA probe decreased 30% upon 1 ng/mL TGF-β addition, and it decreased farther with 2 ng/mL or greater TGF-β addition. Our results are in reasonable agreement with previous studies using rat liver cells, supporting the accuracy of the dsLNA probe for miRNA detection [24].

Our study also demonstrated dynamic measurement of TGF-β-induced miRNA expression in epithelial cells using dsLNA probes. After TGF-β addition, the dsLNA probe measured a miR-21 increase over time for the first two hours. Afterward, the miR-21 signal remained

elevated with a slight gradual decrease over twenty-four hours. Past results have demonstrated a transient increase in miR-21 via TGF-β, with mature miR-21 levels peaking 2- to 10-fold above basal levels at anywhere from two to twenty-four hours after TGF-β addition [27–31]. In the same studies, miR-21 decreased gradually after reaching its peak expression level. These results demonstrate the ability of dsLNA to resolve time-dependent miRNA expression, which is important for studying complex cell regulatory processes.

The dsLNA probe also demonstrated its ability to measure the spatial distribution of miRNA during epithelial collective cell migration. miR-21 is known to regulate proliferation and migration in various cell types [6, 32, 33]. The spatial distribution of miR-21 near the wound edge was revealed by the dsLNA probe in this study. In particular, the gradient of miRNA expression spatially correlated with the expression of β-actin mRNA and the region with reduced cell proliferation, suggesting spatial coordination during epithelial collective cell migration and the involvement of miR-21 in the process. Furthermore, TGF-β stimulation increased the overall miR-21 level while maintaining the spatial gradient in miR-21.

With the spatiotemporal gene distribution realized via the dsLNA probe, our results revealed new insights and questions in the spatiotemporal effects of TGF-β, and its relationship to miR-21 signaling, on MCF-7 epithelial breast cancer cells. In particular, the strategy that the cells collectively maintain the spatial gradient near the leading edge has not been determined and the mechanistic system of miRNA regulation during epithelial collective migration remains largely unknown. TGF-β may influence the complex epithelial migration process by modulating cell proliferation, mobility, and cell-cell interactions, and its effects can also be cell-type dependent [34–37]. TGF-β's anti-proliferative effects coupled to miR-21–induced proliferation have been reported previously [27]. Wang et al. performed miR-21 knockdown experiments along with ectopic, transfected miR-21 expression to elucidate the relationship between miR-21 and TGF-β. They concluded that miR-21 reduces TGF-β-induced growth inhibition in HaCaT cells [27]. This may represent an autoregulatory mechanism in controlling epithelial collective migration. With the increase in miR-21 at the wound edge found from this study, it may be possible that miR-21 regulates the short-term TGF-β-induced reduction in collective migration and proliferation of MCF-7 cells. In addition, MCF-7 cells, unlike HaCaT cells, experience weak epithelial-mesenchymal transition in response to TGF-β addition, which further complicates the overall migratory behaviors [38].

5. Conclusion

This study reports the capability of the dsLNA probes as an effective, applicable method for measuring miRNA levels in living cells. The miRNA distribution observed implies that epithelia toward the leading edge of a monolayer experience either a chemical or physical signal triggering miRNA changes. With the addition of TGF-β, a cytokine related to epithelial-mesenchymal transition, the level of miR-21, regardless of its position near the wound edge, increases. For epithelial wound assays this possibility carries important implications for investigating miRNA's role during drug toxicity studies for cancer or regenerative medicine. The probe can not only measure changes in miRNA over time, but it is also capable of measuring miRNA levels spatially throughout a monolayer—an important characteristic since miRNAs regulate spatial modifications of cell fate. Measuring the spatial

proliferation and migration of MCF-7 cells treated with TGF-β indicates that, in the timeframe utilized in this study, the spatial expression of miR-21 participates in short-term TGF-β modulated epithelial collective migration. Overall, the dsLNA probe is a diverse research tool whose characteristics are advantageous in a variety of laboratory techniques, including cell and tissue differentiation or cancer progression analysis.

Supplementary Material

Refer to Web version on PubMed Central for supplementary material.

Acknowledgments

This work is supported by NIH Director's New Innovator Award (1DP2OD007161-01).

References

1. Kozomara A, Griffiths-Jones S. miRBase: integrating microRNA annotation and deep-sequencing data. Nucleic Acids Res. 2011; 39:D152–7. [PubMed: 21037258]
2. He L, Hannon GJ. MicroRNAs: small RNAs with a big role in gene regulation. Nat Rev Genet. 2004; 5:522–31. [PubMed: 15211354]
3. Wang T, Feng Y, Sun H, Zhang L, Hao L, Shi C, et al. miR-21 regulates skin wound healing by targeting multiple aspects of the healing process. The American journal of pathology. 2012; 181:1911–20. [PubMed: 23159215]
4. Au Yeung CL, Tsang TY, Yau PL, Kwok TT. Human papillomavirus type 16 E6 induces cervical cancer cell migration through the p53/microRNA-23b/urokinase-type plasminogen activator pathway. Oncogene. 2011; 30:2401–10. [PubMed: 21242962]
5. Ham O, Song BW, Lee SY, Choi E, Cha MJ, Lee CY, et al. The role of microRNA-23b in the differentiation of MSC into chondrocyte by targeting protein kinase A signaling. Biomaterials. 2012; 33:4500–7. [PubMed: 22449550]
6. Yang X, Wang J, Guo S-L, Fan K-J, Li J, Wang Y-L, et al. miR-21 promotes keratinocyte migration and re-epithelialization during wound healing. Int J Biol Sci. 2011; 7:685–90. [PubMed: 21647251]
7. Wang J, Wang Y, Wang Y, Ma Y, Lan Y, Yang X. Transforming growth factor β-regulated microRNA-29a promotes angiogenesis through targeting the phosphatase and tensin homolog in endothelium. The Journal of biological chemistry. 2013; 288:10418–26. [PubMed: 23426367]
8. Dong H, Lei J, Ju H, Zhi F, Wang H, Guo W, et al. Target-cell-specific delivery, imaging, and detection of intracellular microRNA with a multifunctional SnO2 nanoprobe. Angew Chem Int Ed Engl. 2012; 51:4607–12. [PubMed: 22473624]
9. van Rooij E. The art of microRNA research. Circ Res. 2011; 108:219–34. [PubMed: 21252150]
10. Riahi R, Dean Z, Wu T-H, Teitell Ma, Chiou P-Y, Zhang DD, et al. Detection of mRNA in living cells by double-stranded locked nucleic acid probes. Analyst. 2013; 138:4777–85. [PubMed: 23772441]
11. Gidwani V, Riahi R, Zhang DD, Wong PK. Hybridization kinetics of double-stranded DNA probes for rapid molecular analysis. Analyst. 2009; 134:1675–81. [PubMed: 20448937]
12. Riahi R, Mach KE, Mohan R, Liao JC, Wong PK. Molecular detection of bacterial pathogens using microparticle enhanced double-stranded DNA probes. Analytical chemistry. 2011; 83:6349–54. [PubMed: 21718053]
13. Meserve D, Wang Z, Zhang DD, Wong PK. A double-stranded molecular probe for homogeneous nucleic acid analysis. Analyst. 2008; 133:1013–9. [PubMed: 18645642]
14. Kang WJ, Cho YL, Chae JR, Lee JD, Choi KJ, Kim S. Molecular beacon-based bioimaging of multiple microRNAs during myogenesis. Biomaterials. 2011; 32:1915–22. [PubMed: 21122913]

15. Kim JK, Choi KJ, Lee M, Jo MH, Kim S. Molecular imaging of a cancer-targeting theragnostics probe using a nucleolin aptamer- and microRNA-221 molecular beacon-conjugated nanoparticle. Biomaterials. 2012; 33:207–17. [PubMed: 21944470]
16. Riahi R, Wang S, Long M, Li N, Chiou PY, Zhang DD, et al. Mapping photothermally induced gene expression in living cells and tissues by nanorod-locked nucleic Acid complexes. Acs Nano. 2014; 8:3597–605. [PubMed: 24645754]
17. Davis S, Lollo B, Freier S, Esau C. Improved targeting of miRNA with antisense oligonucleotides. Nucleic Acids Res. 2006; 34:2294–304. [PubMed: 16690972]
18. Baker MB, Bao G, Searles CD. In vitro quantification of specific microRNA using molecular beacons. Nucleic Acids Res. 2012; 40:e13. [PubMed: 22110035]
19. Fabani MM, Gait MJ. miR-122 targeting with LNA/2′-O-methyl oligonucleotide mixmers, peptide nucleic acids (PNA), and PNA-peptide conjugates. RNA (New York, NY). 2008; 14:336–46.
20. Riahi R, Long M, Yang Y, Dean Z, Zhang DD, Slepian MJ, et al. Single cell gene expression analysis in injury-induced collective cell migration. Integrative biology : quantitative biosciences from nano to macro. 2014; 6:192–202. [PubMed: 24336811]
21. An J, Enomoto A, Weng L, Kato T, Iwakoshi A, Ushida K, et al. Significance of cancer-associated fibroblasts in the regulation of gene expression in the leading cells of invasive lung cancer. J Cancer Res Clin Oncol. 2013; 139:379–88. [PubMed: 23108890]
22. Friedl P, Gilmour D. Collective cell migration in morphogenesis, regeneration and cancer. Nature reviews Molecular cell biology. 2009; 10:445–57.
23. Davis BN, Hilyard AC, Lagna G, Hata A. SMAD proteins control DROSHA-mediated microRNA maturation. Nature. 2008; 454:56–61. [PubMed: 18548003]
24. Yuan B, Dong R, Shi D, Zhou Y, Zhao Y, Miao M, et al. Down-regulation of miR-23b may contribute to activation of the TGF-β1/Smad3 signalling pathway during the termination stage of liver regeneration. FEBS Lett. 2011; 585:927–34. [PubMed: 21354414]
25. Riahi R, Yang YL, Zhang DD, Wong PK. Advances in wound-healing assays for probing collective cell migration. J Lab Autom. 2012; 17:59–65. [PubMed: 22357609]
26. Schneider, Ca; Rasband, WS.; Eliceiri, KW. NIH Image to ImageJ: 25 years of image analysis. Nature Methods. 2012; 9:671–5. [PubMed: 22930834]
27. Wang T, Zhang L, Shi C, Sun H, Wang J, Li R, et al. TGF-β-induced miR-21 negatively regulates the antiproliferative activity but has no effect on EMT of TGF-β in HaCaT cells. Int J Biochem Cell Biol. 2012; 44:366–76. [PubMed: 22119803]
28. Li Q, Zhang D, Wang Y, Sun P, Hou X, Larner J, et al. MiR-21/Smad 7 signaling determines TGF-β1-induced CAF formation. Sci Rep. 2013; 3:2038. [PubMed: 23784029]
29. Yu Y, Wang Y, Ren X, Tsuyada A, Li A, Liu LJ, et al. Context-dependent bidirectional regulation of the MutS homolog 2 by transforming growth factor β contributes to chemoresistance in breast cancer cells. Mol Cancer Res. 2010; 8:1633–42. [PubMed: 21047769]
30. Yao Q, Cao S, Li C, Mengesha A, Kong B, Wei M. Micro-RNA-21 regulates TGF-β-induced myofibroblast differentiation by targeting PDCD4 in tumor-stroma interaction. International journal of cancer Journal international du cancer. 2011; 128:1783–92. [PubMed: 20533548]
31. Zhong X, Chung ACK, Chen H-Y, Meng X-M, Lan HY. Smad3-mediated upregulation of miR-21 promotes renal fibrosis. J Am Soc Nephrol. 2011; 22:1668–81. [PubMed: 21852586]
32. Ji R, Cheng Y, Yue J, Yang J, Liu X, Chen H, et al. MicroRNA expression signature and antisense-mediated depletion reveal an essential role of MicroRNA in vascular neointimal lesion formation. Circ Res. 2007; 100:1579–88. [PubMed: 17478730]
33. Yan LX, Wu QN, Zhang Y, Li YY, Liao DZ, Hou JH, et al. Knockdown of miR-21 in human breast cancer cell lines inhibits proliferation, in vitro migration and in vivo tumor growth. Breast Cancer Res. 2011; 13:R2. [PubMed: 21219636]
34. Sponsel HT, Breckon R, Hammond W, Anderson RJ. Mechanisms of recovery from mechanical injury of renal tubular epithelial cells. Am J Physiol. 1994; 267:F257–64. [PubMed: 8067386]
35. Chapnick DA, Liu X. Leader cell positioning drives wound-directed collective migration in TGF β-stimulated epithelial sheets. 2014

36. Brown, Ka; Aakre, ME.; Gorska, AE.; Price, JO.; Eltom, SE.; Pietenpol, Ja, et al. Induction by transforming growth factor-beta1 of epithelial to mesenchymal transition is a rare event in vitro. Breast Cancer Res. 2004; 6:R215–31. [PubMed: 15084245]

37. Chen H, Tritton TR, Kenny N, Absher M, Chiu JF. Tamoxifen induces TGF-beta 1 activity and apoptosis of human MCF-7 breast cancer cells in vitro. J Cell Biochem. 1996; 61:9–17. [PubMed: 8726350]

38. Moreno-Bueno G, Peinado H, Molina P, Olmeda D, Cubillo E, Santos V, et al. The morphological and molecular features of the epithelial-to-mesenchymal transition. Nat Protoc. 2009; 4:1591–613. [PubMed: 19834475]

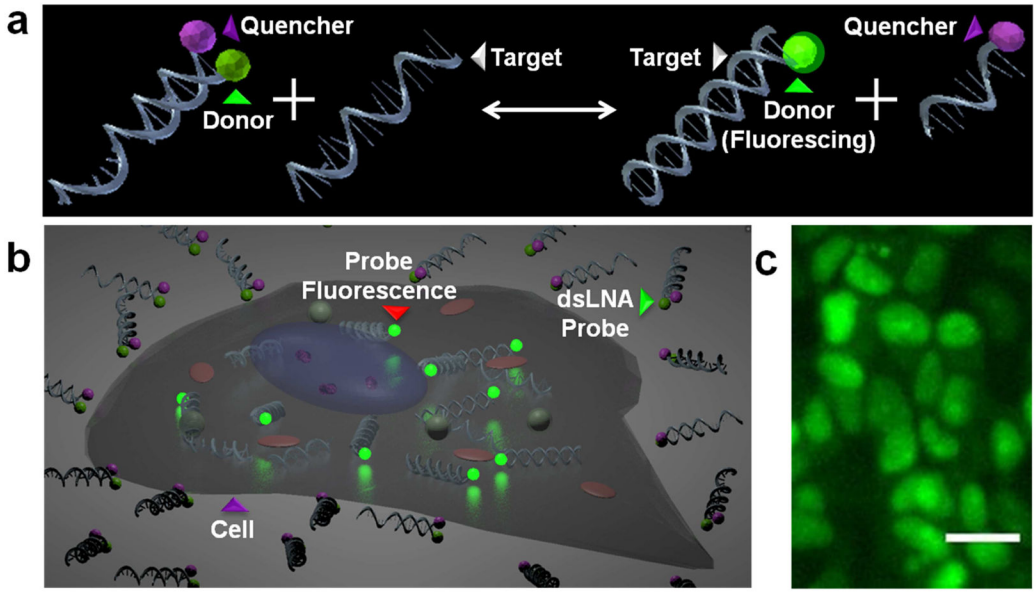

Fig. 1.

dsLNA probe - mechanism of action. (a) Reaction of the dsLNA probe with intracellular target. (b) Illustration demonstrating the dsLNA probes outside a cell versus the dsLNA probes inside a cell, fluorescing when combined with target. (c) Fluorescence image of the dsLNA probe eliciting β-actin mRNA expression in MCF-7 cells. The scale bar is 25 μm.

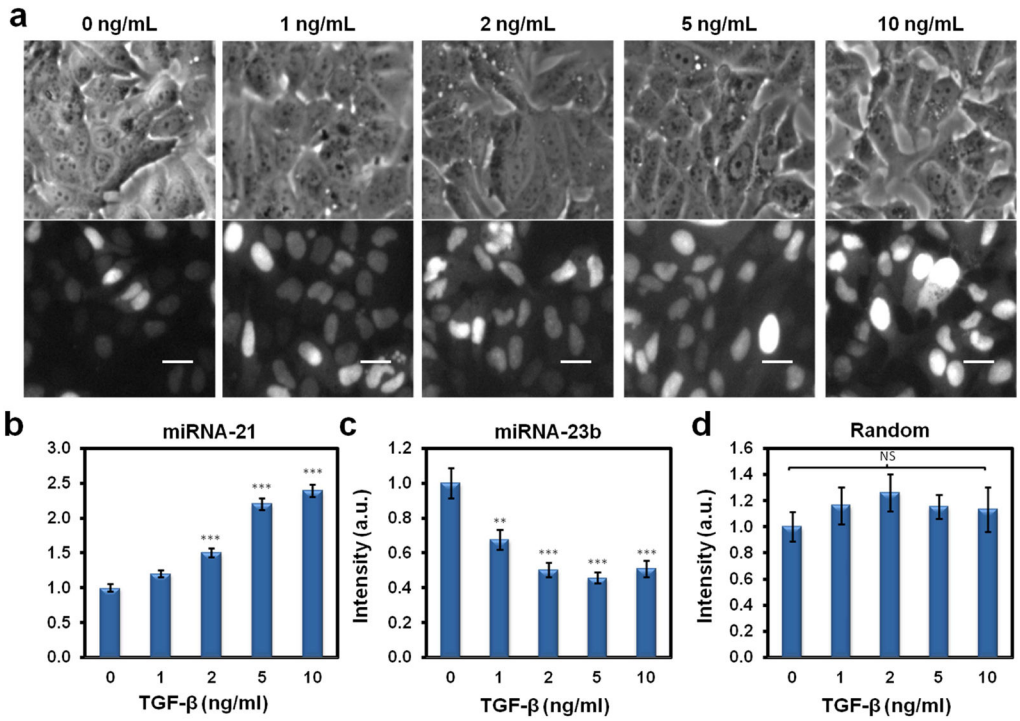

Fig. 2.

TGF-β-induced, dose-dependent increase in miR-21. (a) Bright-field images (top row) and their corresponding fluorescence images (bottom row) illustrating the increase in miR-21 signal seen in the dsLNA probes coinciding with increasing TGF-β concentrations. The scale bars are 25 μm. (b) Graph illustrating the fluorescence intensity of the dsLNA probe to miR-21, showing an increase in signal with increasing TGF-β concentrations. (c) Conversely, the fluorescence intensity of the dsLNA probe to miR-23b decreased with increasing TGF-β concentrations. (d) A random, scrambled dsLNA probe fluorescence signal remained stable with increasing TGF-β concentrations. A one-way ANOVA with Tukey's multiple comparison post-hoc test was performed comparing each dose to the 0 ng/mL TGF-β control (ns, not significant; **, $P<0.01$; ***, $P<0.001$). Changes in random probe signal were not significant regardless of comparison with control or comparison between groups.

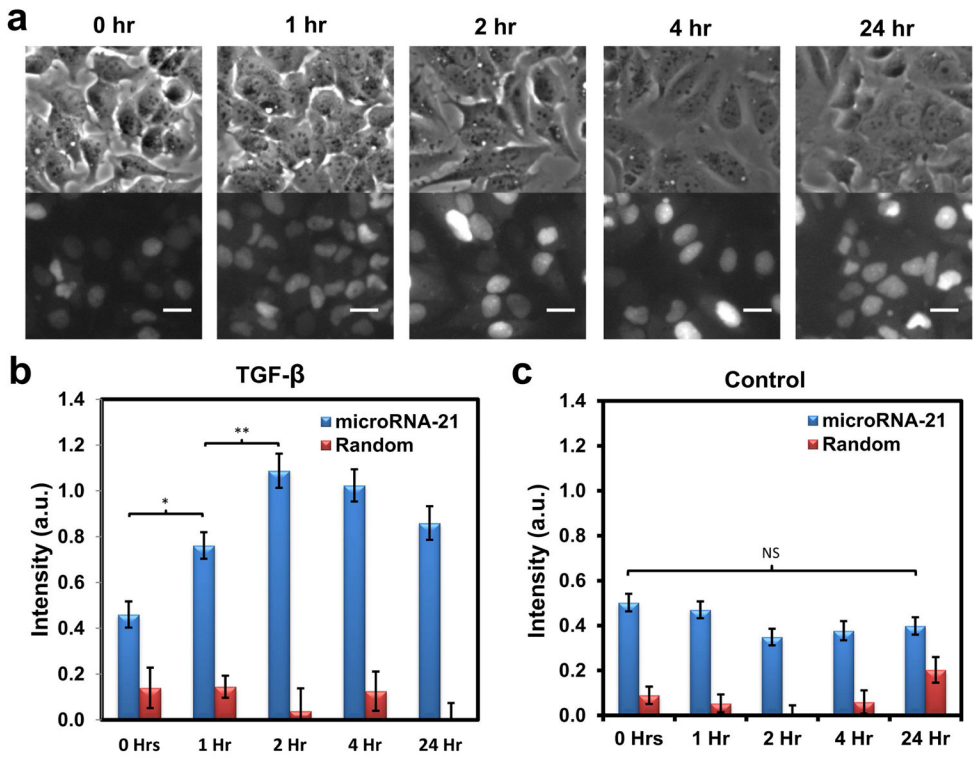

Fig. 3.

TGF-β-induced increase in miR-21 over time. (a) Bright-field images (top row) and their corresponding fluorescence images (bottom row) illustrating the increase in miR-21 signal seen in the dsLNA probes over the first two hours after TGF-β addition. The signal appeared to decrease gradually afterward. (b) Graph illustrating the fluorescence intensity of the dsLNA probe to miR-21 versus a random, scrambled probe over time after TGF-β addition. (c) The experiments were repeated with no TGF-β addition. The miR-21 expression increase over time was significant between the point of TGF-β addition to 1 hour after TGF-β addition (*, $P<0.05$). The miR-21 expression increase over time was also significant between 1 to 2 hours after TGF-β addition (**, $P<0.01$). Without TGF-β addition, no significant change in miR-21 was detected. The miR-21 signal was always statistically significant when compared to the random probe signal, regardless of time or TGF-β dose (***, $P<0.001$). The scale bars are 25 μm.

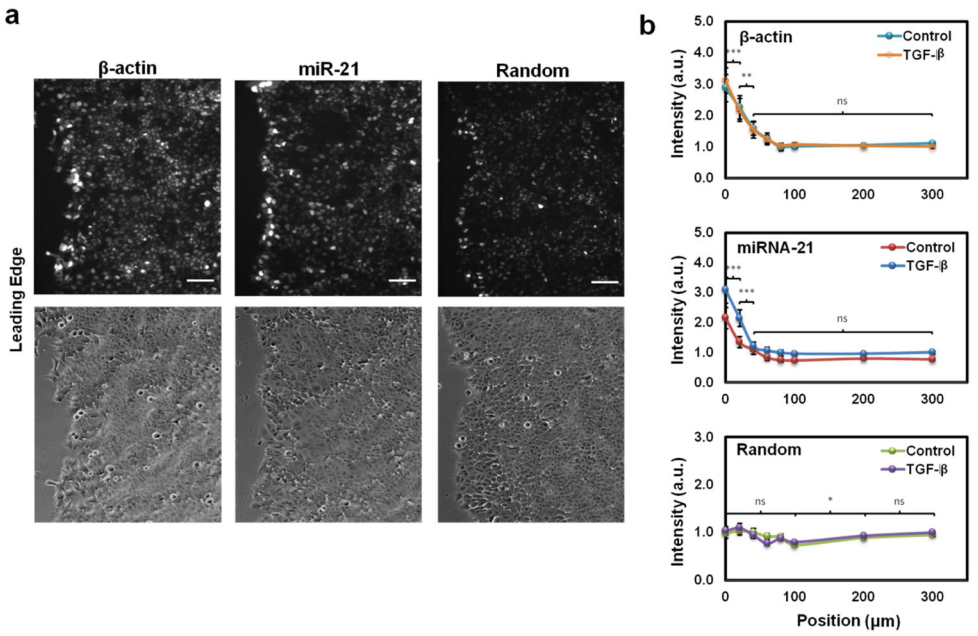

Fig. 4.

Gene expression distribution of a migrating epithelium. (a) Fluorescence images illustrating the distributions of β-actin and miR-21 from the wound edge. The random probe remaind constant regardless of location. (b) Graph displaying the intensity of the β-actin mRNA dsLNA probe as well as the miR-21 dsLNA probe in relation to a scrambled random probe. The experiments were repeated with TGF-β addition. The β-actin probe's fluorescence intensity decreased rapidly over the first 100 μm from the wound edge. The miR-21 probe also decreased during the first 100 μm from the wound edge. The statistical significance indicated on the graphs represents comparisons between points travelling away from the wound edge for the data set where TGF-β was added (***, $P<0.001$; **, $P<0.01$). With TGF-β addition, β-actin and random probes experienced no statistical change, while miR-21 was statistically increased for all distances from the wound edge (***, $P<0.001$) except for 40 μm and 60 μm from the wound edge.

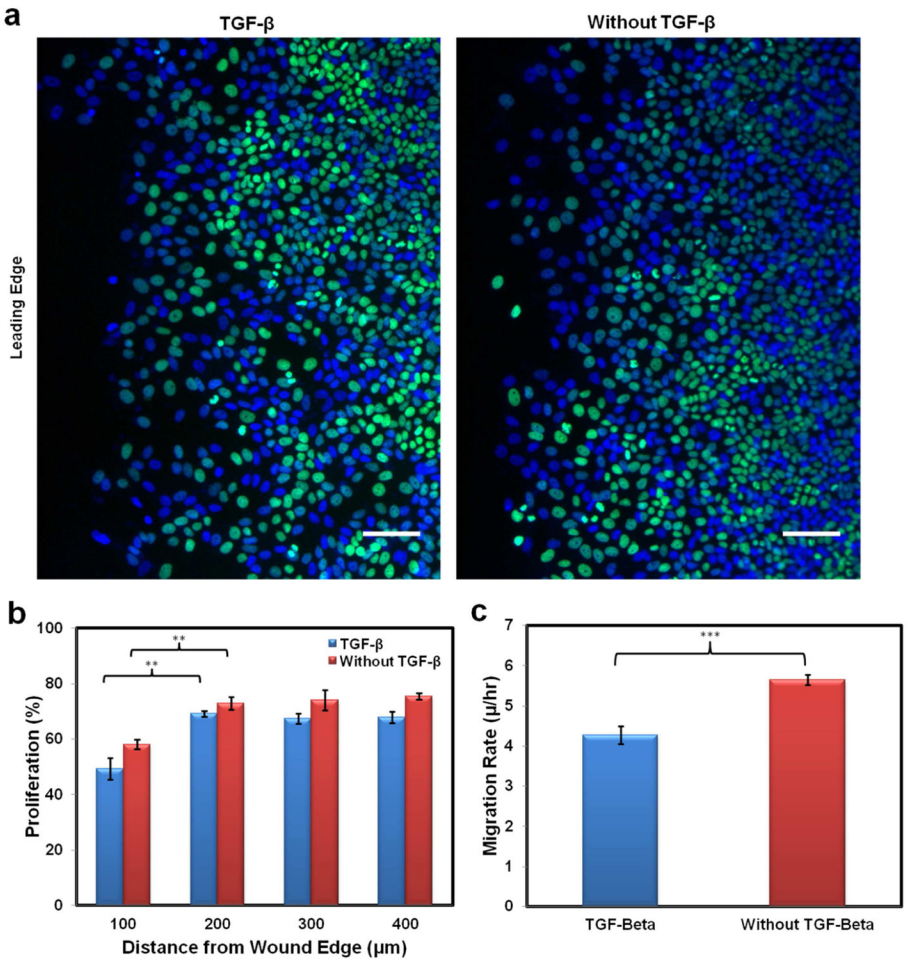

Fig. 5.

Proliferation of migrating MCF-7 cells was measured in a wound healing assay. Proliferation was compared with and without the addition of TGF-β. Over the course of twenty-four hours proliferation inhibition occurred regardless of the vicinity of the cells to the leading edge of the wound. (a) Fluorescence images demonstrating the proliferation measurements. MCF-7 cells were dyed with Hoechst 33342 (blue) and Alexa Fluor 488 (green) via the Click-iT EdU Imaging Kit (Invitrogen). Alexa Fluor 488 presents cells that synthesized DNA over the course of twenty-four hours, while Hoechst 33342 highlights the total number of cells overall. The scale bars are 100 μm. (b) Graph demonstrating the spatial proliferation difference between cells with and without TGF-β addition (**, $P<0.01$). Cells near the wound edge proliferated less than cells in the monolayer, regardless of TGF-β addition. (c) Collective migration of MCF-7 cells in a wound healing assay with and without TGF-β addition. MCF-7 cells grown to confluence were scratched with a pipette tip; this allowed the cells to migrate into the wound area. Migration rate was determined after twenty-four hours of migration by measuring the area covered by the cells over that time and dividing by the width of the monolayer (***, $P<0.001$).

Table 1

A list of sequences for the dsLNA probe strands. The fluorophores are listed in red, with bold, italic, underlined letters indicating LNA bases.

Target RNA	Probe Type	Sequence/Fluorophore
miR-21	Donor(D)	5' /6-FAM/*T*C*A*A*C*A*T*C*A*G*T*C*T*G*A*T*A*A*G*C 3'
	Quencher (Q)	5' *C*T*G*A*T*G*T*T*G*A/Iowa Black RQ/ 3'
	Target Sequence (T)	5′ GCTTATCAGACTGATGTTGA 3′
miR-23b	Donor(D)	5' /6-FAM/*A*T*C*A*G*C*A*T*G*C*C*A*G*G*A*A*C*C*C*A 3'
	Quencher (Q)	5' *G*C*A*T*G*C*T*G*A*T/Iowa Black RQ/ 3'
	Target Sequence (T)	5′ UGGGUUCCUGGCAUGCUGAU 3′
β-actin	Donor(D)	5' /6-FAM/*A*G*G*A*A*G*G*A*A*G*G*C*T*G*G*A*A*G*A*G 3'
	Quencher (Q)	5' *C*T*T*C*C*T*T*C*C*T/Iowa Black RQ/ 3'
	Target (T)	5′ CTCTTCCAGCCTTCCTTCCT 3′
Random	Donor (D)	5' /6-FAM/*A*C*G*C*G*A*C*A*A*G*C*G*C*A*C*C*G*A*T*A 3'
	Quencher (Q)	5' *C*T*T*G*T*C*G*C*G*T/Iowa Black RQ/ 3'
	Target Sequence (T)	5′ TATCGGTGCGCTTGTCGCGT 3′